

**Lithium-Beryllium-Boron Isotopic Compositions in Meteoritic  
Hibonite: Implications for Origin of  $^{10}\text{Be}$  and Early Solar System  
Irradiation**

Ming-Chang Liu

Department of Terrestrial Magnetism, Carnegie Institution of Washington, Washington,  
DC, USA

Institute of Astronomy and Astrophysics, Academia Sinica, Taipei, Taiwan

`mliu@dtm.ciw.edu`

Larry R. Nittler and Conel M. O'D. Alexander

Department of Terrestrial Magnetism, Carnegie Institution of Washington, Washington,  
DC, USA

Typhoon Lee

Institute of Earth Sciences, Academia Sinica, Taipei, Taiwan

Received \_\_\_\_\_; accepted \_\_\_\_\_

## ABSTRACT

NanoSIMS isotopic measurements of Li, Be and B in individual hibonite grains extracted from the Murchison meteorite revealed that  $^{10}\text{B}$  excesses correlate with the  $^9\text{Be}/^{11}\text{B}$  ratios in  $^{26}\text{Al}$ -free PLAty-hibonite Crystals (PLACs). From these data, an initial  $^{10}\text{Be}/^9\text{Be} = (5.5 \pm 1.6) \times 10^{-4}$  ( $2\sigma$ ) and  $^{10}\text{B}/^{11}\text{B} = 0.2508 \pm 0.0015$  can be inferred. On the other hand, chondritic boron isotopic compositions were found in  $^{26}\text{Al}$ -bearing Spinel-HIBonite spherules (SHIBs), most likely due to contamination with normal boron. No  $^7\text{Li}$  excesses due to  $^7\text{Be}$  decay were observed. When combined with previously-reported data, the new data yield the best defined  $^{10}\text{Be}/^9\text{Be} = (5.3 \pm 1.0) \times 10^{-4}$  ( $2\sigma$ ) and  $^{10}\text{B}/^{11}\text{B} = 0.2513 \pm 0.0012$  for PLACs. A comparison of this value and the best constrained  $^{10}\text{Be}/^9\text{Be} = (8.8 \pm 0.6) \times 10^{-4}$  in CV Ca-Al-rich Inclusions (CAIs) supports a heterogeneous distribution of  $^{10}\text{Be}$  and its protosolar irradiation origin. We consider two possible irradiation scenarios that could potentially lead to the observed Li-Be-B isotopic compositions in PLACs. Although *in situ* irradiation of solids with hibonite chemistry seems to provide the simplest explanation, more high quality data will be needed for quantitatively constraining the irradiation history.

*Subject headings:* cosmic rays — meteorites, meteors, meteoroids — nuclear reactions, nucleosynthesis, abundances

## 1. Introduction

Short-lived radionuclides ( $t_{1/2} \lesssim 100$  Myr) in the early Solar System provide important information about the astrophysical environment in which the Solar System formed. Among the short-lived radioactivities whose prior existence has been inferred in meteorites,  $^{10}\text{Be}$  (decays to  $^{10}\text{B}$ ,  $t_{1/2} = 1.5$  Myr) and  $^7\text{Be}$  (decays to  $^7\text{Li}$ ,  $t_{1/2} = 53$  days) are the two that exclusively require an irradiation origin (e.g. Fowler et al. 1961). The stable isotopes of Li, Be and B are also made by irradiation, and the isotopic compositions of these elements are strongly energy dependent (Ramaty et al. 1996). Thus, a quantitative understanding of the initial abundances and distributions of  $^{10}\text{Be}$  and  $^7\text{Be}$ , as well as the stable Li-Be-B isotopic compositions, would provide important constraints on the irradiation environment and processes in the solar nebula.

It is now well established that live  $^{10}\text{Be}$  was present in various types of refractory inclusions when they formed, and that these inclusions had a range of inferred abundances of another short-lived radionuclide,  $^{26}\text{Al}$ . The inferred  $^{10}\text{Be}/^9\text{Be}$  ratios range from  $(3\text{--}4)\times 10^{-4}$  up to  $18\times 10^{-4}$ , albeit with significant analytical errors in most cases (McKeegan et al. 2000; Sugiura et al. 2001; Marhas et al. 2002; MacPherson et al. 2003). Amongst  $^{26}\text{Al}$ -bearing ( $^{26}\text{Al}/^{27}\text{Al} \sim 5\times 10^{-5}$ ) CV-chondrite Ca-Al-rich Inclusions (CAIs), the best constrained initial  $^{10}\text{Be}/^9\text{Be} = (8.8\pm 0.6)\times 10^{-4}$  ( $2\sigma$ ) was reported by Chaussidon et al. (2006a). For  $^{26}\text{Al}$ -free ( $^{26}\text{Al}/^{27}\text{Al} \lesssim 3\times 10^{-6}$ ) inclusions, the most precise  $^{10}\text{Be}/^9\text{Be}$  ratio of  $(5.1\pm 1.4)\times 10^{-4}$  ( $2\sigma$ ) was obtained in a subset of CM-chondrite hibonite ( $\text{CaAl}_{12}\text{O}_{19}$ ) grains, referred to as PLATy hibonite Crystals (PLACs) (Liu et al. 2009a). The  $^{10}\text{Be}/^9\text{Be}$  ratios in other  $^{26}\text{Al}$ -free objects are consistent with this value (Marhas et al. 2002; MacPherson et al. 2003; Marhas & Goswami 2003).

Beryllium-10 and  $^7\text{Be}$  are primarily produced through the same nucleosynthetic pathway, namely  $^{16}\text{O}(p, x)$ . Consequently, refractory inclusions where  $^{10}\text{Be}$  was found might

be expected to also contain  ${}^7\text{Be}$ . However, because of the complicated chemical and isotopic behavior of Li (e.g., Chaussidon et al. 2006b), whether  ${}^7\text{Be}$  existed in refractory inclusions is still an open question. The only hint for the existence of  ${}^7\text{Be}$  ( ${}^7\text{Be}/{}^9\text{Be} = (6.1 \pm 1.3) \times 10^{-3}$ ) in the solar nebula was reported by Chaussidon et al. (2006a). Further surveys for  ${}^7\text{Be}$  are needed for confirmation of its presence, and for a better understanding of its initial abundance and distribution in the solar nebula.

Live  ${}^{10}\text{Be}$  in the early Solar System could have formed as a consequence of protosolar irradiation, with variable abundances in different objects arising from varied irradiation histories (e.g., McKeegan et al. 2000; Marhas et al. 2002; MacPherson et al. 2003; Chaussidon et al. 2006a; Liu et al. 2009a). Alternatively, trapping of  ${}^{10}\text{Be}$ -enriched Galactic Cosmic Rays (GCRs) by the magnetic fields of the progenitor molecular cloud core has been proposed as a source of  ${}^{10}\text{Be}$  (Desch et al. 2004). In this scenario, a uniform initial  ${}^{10}\text{Be}/{}^9\text{Be}$  ratio would exist in the solar nebula, which would allow  ${}^{10}\text{Be}$  to be used for chronometry. However, since  ${}^{26}\text{Al}$  appears to be a valid chronometer (Villeneuve et al. 2009), a comparison between  ${}^{26}\text{Al}$ -bearing CAIs and  ${}^{26}\text{Al}$ -free PLACs suggests that the difference in  ${}^{10}\text{Be}/{}^9\text{Be}$  has no chronological meaning, making irradiation in the solar nebula the likely source of most of the  ${}^{10}\text{Be}$  (Liu et al. 2009a).

The above argument that  ${}^{10}\text{Be}$  had a protosolar irradiation origin is based on a chronological viewpoint. If one aims to quantitatively understand the spatial distribution of  ${}^{10}\text{Be}$  in a certain time period, examination of different objects that formed closely in time is needed. The available CAI  ${}^{10}\text{Be}$  data appear to show some heterogeneity, but there are large analytical uncertainties (e.g. McKeegan et al. 2000; Sugiura et al. 2001; MacPherson et al. 2003). CM-chondrite Spinel-HIBonite spherules (SHIBs) would be a good alternative target for investigating  ${}^{10}\text{Be}$  heterogeneity, as their inferred  ${}^{26}\text{Al}/{}^{27}\text{Al}$  ratios indicate that they probably formed  $\sim 1 \times 10^5$  years after CAIs (Liu et al. 2009a), and the change in  ${}^{10}\text{Be}$

abundances due to radioactive decay over this time period would have been negligible. However, resolvable  $^{10}\text{B}$  excesses have not yet been found in SHIBs, primarily because of pervasive B contamination from surface cracks and the lack of uniform areas in these objects that are large enough to contain a typical ion microprobe spot ( $\sim 30 - 50\mu\text{m}$ ; e.g., Liu et al. 2009a). These problems can be overcome to some degree with the higher spatial resolution of the Cameca NanoSIMS ion probe. Here we report the results of Li-Be-B isotopic measurements in CM hibonites obtained with the CIW NanoSIMS 50L, and discuss their astrophysical implications.

## 2. Experimental

Hibonite grains were hand-picked from an acid residue of the Murchison meteorite (courtesy of Andy Davis, the University of Chicago). Of the 40 hibonite samples found, only 9 grains (2 SHIBs and 7 PLACs) that had large enough areas of hibonite ( $\sim 20 - 60\mu\text{m}$  across) were selected for measurements.

For the Li-Be-B measurements, a 5 nA, 16 KeV  $^{16}\text{O}^-$  primary beam ( $\phi \sim 7 - 10\mu\text{m}$ ) was used to generate a  $\sim 15 \times 15 \mu\text{m}^2$  raster square on polished, epoxy-mounted samples. Secondary ions ( $^6\text{Li}^+$ ,  $^7\text{Li}^+$ ,  $^9\text{Be}^+$ ,  $^{10}\text{B}^+$ ,  $^{11}\text{B}^+$ ,  $^{27}\text{Al}^{++}$ ) were counted simultaneously with six electron multipliers (EMs). Beam blanking was applied in every analysis, so that only signals from the central  $6 \times 6 \mu\text{m}^2$  area were collected. Before each measurement, samples were pre-sputtered for 5–10 minutes until the B signal became steady. The mass resolution was sufficient to resolve isobaric interferences. Counting times were optimized based on the  $^{10}\text{B}$  count rate ( $\ll 1 - \sim 10 \text{ counts sec}^{-1}$ ) to reach sufficient counting statistics with the resulting total analysis times of 1.5 – 3 hours. Sample charging was monitored and corrected for every 30 cycles. The data were also corrected for EM background ( $\sim 0.003 \text{ counts sec}^{-1}$ ). Under such low count rates, the analytical uncertainties were primarily

determined by counting statistics.

The instrumental mass fractionation (IMF) and relative sensitivity factors (RSFs), which relate measured secondary ion ratios to true concentration ratios, were determined from measurements of an NBS612 glass ( $^{10}\text{B}/^{11}\text{B} = 0.2469$ ;  $^9\text{Be}/^{11}\text{B} = 1.79$ ; Kasemann et al. 2001;  $^7\text{Li}/^6\text{Li} = 12.3918$ ;  $^9\text{Be}/^6\text{Li} = 9.41^1$ ). The Li, Be and B concentrations of the samples were estimated by comparison with the NBS612 glass ( $[\text{Li}] = 41.8$  ppm,  $[\text{Be}] = 38.3$  ppm and  $[\text{B}] = 32$  ppm; Pearce et al. 1997) with the equation:

$$[x]_{\text{sample}} = \frac{(Al^{++})_{std}^m}{(x)_{std}^m} \times \frac{(x)_{\text{sample}}^m}{(Al^{++})_{\text{sample}}^m} \times \frac{[x]_{std}}{[Al_2O_3]_{std}} \times [Al_2O_3]_{\text{sample}}$$

where  $x$  represents Li, Be or B, and the superscript  $m$  represents measured. It should be pointed out that differences in IMFs and RSFs between silicate glasses and oxides could exist. Contributions from spallogenic  $^6\text{Li}$ ,  $^7\text{Li}$ ,  $^9\text{Be}$ ,  $^{10}\text{B}$ , and  $^{11}\text{B}$  in hibonite samples by GCR irradiation of the host meteorite were also estimated by adopting an exposure age of 1.8 My for the Murchison meteorite (Herzog et al. 1997). However, they were insignificant compared to the analytical errors.

### 3. Results

The Li and B isotopic compositions and elemental concentrations of the measured grains are reported in Table 1. Literature data from Liu et al. (2009a) are also listed for comparison. The  $^9\text{Be}/^6\text{Li}$  and  $^9\text{Be}/^{11}\text{B}$  ratios in the new grains both span a wide range, from slightly higher than the chondritic values (0.18 and 0.053, respectively; Lodders 2003) to a few hundred, but are less extreme than those reported by Liu et al. (2009a). Resolvable  $^{10}\text{B}$  excesses correlating with the  $^9\text{Be}/^{11}\text{B}$  ratios are found in a suite of hibonite

---

<sup>1</sup>lithium data: [http://www.geol.umd.edu/pages/facilities/li\\_analytical.pdf](http://www.geol.umd.edu/pages/facilities/li_analytical.pdf)

grains, indicating the *in situ* decay of  $^{10}\text{Be}$ . The best fit through all the points yields a slope corresponding to  $^{10}\text{Be}/^9\text{Be} = (5.5 \pm 1.6) \times 10^{-4}$  ( $2\sigma$ ), with an intercept  $^{10}\text{B}/^{11}\text{B} = 0.2508 \pm 0.0015$  (Figure 1). Although this correlation line is primarily defined by the two highest points on the sample mt3-P13, the  $\bar{\chi}^2 = 0.9$  indicates that all the hibonite grains could have sampled a common  $^{10}\text{Be}$  reservoir. This result corroborates the previous work of Marhas et al. (2002) and Liu et al. (2009a). If we combine the NanoSIMS results with those of Liu et al. (2009a),  $^{10}\text{Be}/^9\text{Be} = (5.3 \pm 1.0) \times 10^{-4}$  and  $^{10}\text{B}/^{11}\text{B} = 0.2513 \pm 0.0012$  ( $\bar{\chi}^2 = 1.1$ ) can be inferred from the best fit (Figure 2). This  $^{10}\text{Be}/^9\text{Be}$ , so far the most precise initial ratio for CM PLACs, is  $\sim 40\%$  lower than the best constrained value  $(8.8 \pm 0.6) \times 10^{-4}$  for CV CAIs, whereas the initial  $^{10}\text{B}/^{11}\text{B}$  ratios for the two groups of objects agree with each other within errors, and are  $\sim 1.5\%$  higher than the chondritic value ( $= 0.2476$ , Zhai et al. 1996). Unfortunately, we were unable to detect resolvable  $^{10}\text{B}$  excesses in SHIBs, even if they were present at the levels seen in PLACs, because SHIBs have much lower Be/B ratios than do PLACs.

The  $^7\text{Li}/^6\text{Li}$  ratios in these grains do not show any evidence for  $^7\text{Be}$  decay, and are all consistent within the uncertainties with the chondritic value (12.02, McDonough et al. 2003). The best fit results in  $^7\text{Be}/^9\text{Be} = (0.6 \pm 2) \times 10^{-4}$  ( $2\sigma$ ) and  $^7\text{Li}/^6\text{Li} = 12.01 \pm 0.02$  (Figure 3), indicating that these grains were grossly contaminated by terrestrial/chondritic Li, were isotopically disturbed, or formed without  $^7\text{Be}$ . When combined with the Li data from Liu et al. (2009a), it is clear that all hibonite grains are characterized by chondritic  $^7\text{Li}/^6\text{Li}$ , with only a few exceptions showing resolvably lower ratios.

The Li, Be, and B concentrations of the samples range from a few ppb to hundreds of ppb, similar to what was observed by Liu et al. (2009a). An interesting observation, although based on somewhat limited amounts of data, is that PLACs that define the Be-B correlation line (Mur-P1, Mur-P7, Mur-P8, Mur-P9, mt3-P4, mt3-P13, and mt4-P4) all

have similar [Be]  $\sim 600 \pm 100$  ppb, whereas SHIBs tend to have much lower [Be], only  $\sim 20 - 60$  ppb.

## 4. Discussion

### 4.1. Protosolar irradiation origin for $^{10}\text{Be}$

Because  $^{10}\text{Be}$  is destroyed in stellar nucleosynthesis, its presence in the early Solar System requires nuclear reactions with energetic particles (e.g., McKeegan et al. 2000; Marhas et al. 2002; Chaussidon et al. 2006a; Liu et al. 2009a). Two mainstream models responsible for the origin of  $^{10}\text{Be}$  include *in situ* irradiation from the proto-Sun (e.g., Gounelle et al. 2001, 2006) and the trapping of GCR- $^{10}\text{Be}$  by the molecular cloud core (Desch et al. 2004). The inferred  $^{10}\text{Be}$  abundance in CM PLACs, which have been thought to have formed without live  $^{26}\text{Al}$  because they are devoid of  $^{26}\text{Mg}$  excesses or even have apparent  $^{26}\text{Mg}$  deficits (e.g., Liu et al. 2009a), sheds light on the origin of  $^{10}\text{Be}$ . The  $^{10}\text{Be}/^9\text{Be}$  value of  $(5.3 \pm 1.0) \times 10^{-4}$  in CM PLACs reinforces the argument made by Liu et al. (2009a) that GCR-trapping is unlikely to be the dominant source of  $^{10}\text{Be}$ . Assuming chronological significance for  $^{10}\text{Be}$ , the difference in formation time between  $(5.3 \pm 1.0) \times 10^{-4}$  (PLACs) and  $(8.8 \pm 0.6) \times 10^{-4}$  (CAIs, Chaussidon et al. 2006a) ranges from 0.6 to 1.7 My. However, this age difference would predict that the PLAC  $^{26}\text{Al}/^{27}\text{Al}$  should have been between  $\sim (1 - 3) \times 10^{-5}$ , much higher than observed. Alternatively, as argued by Liu et al. (2009a), the lack of  $^{26}\text{Al}$  found in PLACs could not be explained by late formation, but might have been the result of formation prior to a late injection of  $^{26}\text{Al}$  and formation of CAIs (Sahijpal & Goswami 1998). In this case, PLACs should have at least the same, or higher,  $^{10}\text{Be}/^9\text{Be}$  than CV CAIs if GCR-trapping was the primary source of  $^{10}\text{Be}$ . Therefore, the  $^{10}\text{Be}/^9\text{Be}$  difference between PLACs and CAIs cannot be explained chronologically, and  $^{10}\text{Be}$  must not have been homogeneously distributed in the inner

solar nebula. Another line of evidence comes from the initial  $^{10}\text{B}/^{11}\text{B}$  ratio. The initial ratios for PLACs ( $0.2513 \pm 0.0012$ ) and for Allende CV CAIs ( $0.2538 \pm 0.0015$ ; Chaussidon et al. 2006a) agree within error. These  $^{10}\text{B}/^{11}\text{B}$  ratios are too high to be explained by a widespread decay of  $^{10}\text{Be}$  in a gas of solar composition ( $\text{Be}/\text{B} = 0.04$ ). Instead, their supra-chondritic  $^{10}\text{B}/^{11}\text{B}$  ratios are best understood as a mixture between chondritic and spallogenic B. From all these observations, we conclude that  $^{10}\text{Be}$  was produced by *in situ* protosolar irradiation.

Similar to previous studies,  $^{10}\text{B}$  excesses could not be resolved in SHIBs. Even though we were able to analyze almost pure hibonite, low  $^9\text{Be}/^{11}\text{B}$  ratios ( $<1$ ) due to low  $[\text{Be}]$  and high  $[\text{B}]$  would have obscured any  $^{10}\text{B}$  excesses, if present. The low Be concentrations ( $\sim 10\times$  lower than that in PLACs) might be because SHIBs crystallized from a Be-depleted precursor melt, whereas high  $[\text{B}]$  could have been due to the introduction of “common B” into SHIBs during either crystallization, or later alteration along cracks. Therefore, meaningful comparisons of  $^{10}\text{Be}/^9\text{Be}$  between  $^{26}\text{Al}$ -bearing SHIBs and CAIs still remain impossible.

#### 4.2. Implications for early Solar System irradiation

In principle, the Li-Be-B isotopic compositions of the oldest refractory solids could serve as good probes of irradiation processes in the earliest stages of the Solar System. In hibonites, unfortunately, only the  $^{10}\text{Be}$ - $^{10}\text{B}$  system is defined well enough to provide such constraints. Thus, here we consider two possible irradiation scenarios: irradiation of hibonite solids and irradiation of solar gas, with the primary goal of reconstructing the observed Be-B isotopic results in PLACs, and subsequently assessing the possible collateral results for Li isotopes. Both cases share the assumption that only proton irradiation was involved, so that collaterally produced  $^{26}\text{Al}$  (from  $^{27}\text{Al}(p, pn)^{26}\text{Al}$ ) would not exceed

the inferred abundances in PLACs ( $^{26}\text{Al}/^{27}\text{Al} \lesssim 3 \times 10^{-6}$ ) (Gounelle et al. 2006; Liu & McKeegan 2009b). The cross sections of relevant reactions are either taken from Sisterson et al. (1997) and Michel et al. (1997), or calculated with the TALYS code (Koning et al. 2005).

#### 4.2.1. Irradiation of solid hibonite

In this scenario, there was *in-situ* irradiation of already-formed hibonite grains near the proto-Sun (Liu & McKeegan 2009b). At the cessation of condensation, hibonite would contain Be but should be essentially free of Li and B, as they do not condense until  $T \lesssim 1100$  K (e.g., Lodders 2003). Assuming an initial  $[\text{Be}] = 500$  ppb in the solids, which is roughly an average in the grains that define the Be-B correlation line, and a proton fluence that produces  $^{10}\text{Be}/^9\text{Be} = 5.3 \times 10^{-4}$ , we obtain the following isotopic ratios in hibonite at the end of the irradiation:  $^{10}\text{B}/^{11}\text{B} \sim 0.44$  (the ratio of cross sections of  $^{16}\text{O}(p, x)^{10,11}\text{B}$  measured at 135 MeV; Yiou et al. 1968),  $^9\text{Be}/^{11}\text{B} \sim 11$ ,  $^7\text{Be}/^9\text{Be} \sim 3 \times 10^{-4}$ ,  $^7\text{Li}/^6\text{Li} \sim 0.8$  (the same method as for B), and  $^9\text{Be}/^6\text{Li} \sim 27$ . The Li and B isotopic ratios do not include any radiogenic components from the decay of  $^7\text{Be}$  and  $^{10}\text{Be}$ , respectively.

This simple calculation shows that if grains were irradiated *in situ*, the Li-Be-B isotopic compositions seen in PLACs cannot be purely spallogenic, but instead require spallation followed by partial loss of spallogenic Li and B, and isotopic exchange with a chondritic gas. The measured initial  $^{10}\text{B}/^{11}\text{B} = 0.2513$  for PLACs is much lower than the pure spallogenic ratio 0.44, indicating that the grains must have experienced post-irradiation isotope exchange with a chondritic reservoir(s) ( $^{10}\text{B}/^{11}\text{B} = 0.2476$ ), and only  $\sim 2\%$  of the pure spallogenic component was preserved. The exchange would have to have taken place after a diffusive loss of spallogenic B from the grains (B is unstable in refractory phases at high temperatures), but before  $^{10}\text{Be}$  had decayed significantly, so that the grains would

have variable  $^9\text{Be}/^{11}\text{B}$  ratios and the same starting  $^{10}\text{B}/^{11}\text{B} = 0.2513$ . This explains why PLACs form a well-defined Be-B correlation line. The variation in  $^9\text{Be}/^{11}\text{B}$  might simply reflect different degrees of B loss when the exchange with chondritic matter occurred. It is important to note that CV CAIs could have derived their Be-B isotopic characteristics in this scenario, if their refractory precursors were also B-free.

The above processes would probably affect the Li isotopic system in a similar way, since Li and B have similar volatility. However, the high mobility of Li at high temperatures (e.g., Coogan et al. 2005) and fast decay rate of  $^7\text{Be}$  greatly complicated the Li isotopic evolution in hibonite. Qualitatively, the lower-than-chondritic  $^7\text{Li}/^6\text{Li}$  in some hibonite grains (Mur-S15, Mur-P6, Mur-P8 and Mur-P9, Liu et al. 2009a) could be explained by mixing pure spallogenic Li ( $^7\text{Li}/^6\text{Li} \sim 0.8$ ) with chondritic components ( $^7\text{Li}/^6\text{Li} = 12.02$ ). A quantitative evaluation of how Li isotopes evolved in the grains still requires a detailed understanding of Li diffusion in hibonite and residence time at high temperatures, on which we still lack constraints.

#### 4.2.2. Irradiation of solar gas

In this scenario, proton irradiation of nebular gas was followed by condensation of hibonites. The initial gas composition is taken as the solar composition of Lodders (2003), with the starting  $^7\text{Li}/^6\text{Li} = 12.26$  and  $^{10}\text{B}/^{11}\text{B} = 0.2472$ . It should be pointed out that the  $^7\text{Li}/^6\text{Li}$  and  $^{10}\text{B}/^{11}\text{B}$  from Lodders (2003) are slightly different from the measured ones of McDonough et al. (2003) and Zhai et al. (1996), respectively, but we can ignore this discrepancy since it does not have any impact on the conclusion. We estimate the final  $^{10}\text{Be}/^9\text{Be}$ ,  $^7\text{Be}/^9\text{Be}$ ,  $^7\text{Li}/^6\text{Li}$ , and  $^{10}\text{B}/^{11}\text{B}$  in the gas parcel in which hibonite formed, despite the fact that Li and B would not condense into the solids at the condensation temperatures of hibonite. The production of Li-Be-B isotopes was calculated by considering spallation

on  $^{12}\text{C}$ ,  $^{14}\text{N}$  and  $^{16}\text{O}$ . The result shows that for a proton fluence that produces  $^{10}\text{Be}/^9\text{Be} = 5.3 \times 10^{-4}$ ,  $^7\text{Be}/^9\text{Be}$ ,  $^7\text{Li}/^6\text{Li}$  and  $^{10}\text{B}/^{11}\text{B}$  would be at the level of  $\sim 8 \times 10^{-3}$ , 12.26 and 0.2473, respectively. The condensed hibonite could have incorporated  $^{10}\text{Be}$  at this abundance, but the amount of incorporated  $^7\text{Be}$  would strongly depend on the time delay between the termination of irradiation and hibonite formation. This means that the lack of radiogenic  $^7\text{Li}$  excesses in PLACs could be explained in this scenario if they had formed  $>1$  year after irradiation.

One challenge for this explanation is to reproduce the initial  $^{10}\text{B}/^{11}\text{B} = 0.2513$ . Freshly formed CM PLACs would be free of B. For PLACs to acquire a ratio of 0.2513, one has to invoke a supra-chondritic B component. Nebular gas near the proto-Sun would have been the most likely candidate because its  $^{10}\text{B}/^{11}\text{B}$  could be elevated by solar energetic particle spallation more easily than that of the Murchison parent body. However, as shown above, to raise the  $^{10}\text{B}/^{11}\text{B}$  to 0.2513 in a solar gas, the collateral  $^{10}\text{Be}/^9\text{Be}$  ratio would have to be much higher than observed (e.g.,  $\sim 3 \times 10^{-2}$ ). In addition, given a high mixing efficiency in a marginally gravitationally unstable disk (e.g., Boss 2008), whether a supra-chondritic gaseous reservoir could have lasted long enough to interact with PLACs is a question. Another potential problem with this scenario, although it can be very model dependent, is that even if grains exchanged B isotopes with supra-chondritic gas, possible secondary processing in the meteorite parent body could still introduce “normal” B into the PLACs and lower their  $^{10}\text{B}/^{11}\text{B}$  ratios. Because grains could have experienced various degrees of parent body processing, and thus mixed with various proportions of chondritic B, it would require multiple supra-chondritic components of different  $^{10}\text{B}/^{11}\text{B}$  in the gas and ad-hoc mixing ratios to explain a well-defined initial ratio in PLACs. From this view, irradiation of solar gas seems less likely to be responsible for  $^{10}\text{Be}$  and  $^7\text{Be}$  in the early Solar System. It should also be noted that isotopic fractionation associated with recondensation of normal gas onto the grain surface could potentially lead to enrichment of  $^{10}\text{B}$ ; however at this point

the evidence for this process occurring in the solar nebula is still lacking.

## 5. Conclusion

Combining new NanoSIMS measurements of  $^{26}\text{Al}$ -free platy hibonite crystals (PLACs) with the results of Liu et al. (2009a) yields, as of now, the best defined initial  $^{10}\text{Be}/^9\text{Be}$  ratio of  $(5.3\pm 1.0)\times 10^{-4}$  and initial  $^{10}\text{B}/^{11}\text{B} = 0.2513\pm 0.0012$  for CM PLACs. This result reinforces the argument against the model that observed  $^{10}\text{Be}$  in early Solar System objects originated as trapped GCR material, and thus supports a protosolar irradiation origin for  $^{10}\text{Be}$ . As in previous studies, we failed to find resolvable  $^{10}\text{B}$  excesses in  $^{26}\text{Al}$ -bearing SHIBs, so that a meaningful comparison with CAIs on initial  $^{10}\text{Be}/^9\text{Be}$  ratios remains impossible. Both irradiation of hibonite solids and of solar gas could qualitatively lead to the observed Li-Be-B isotopic compositions; however, the former provides a simpler explanation. To quantitatively constrain the irradiation history of CM hibonites, more data, especially higher quality Li isotopic measurements, are needed.

The authors thank the referee for invaluable comments, Kevin McKeegan for inspiring discussion, Andy Davis for providing a Murchison residue, and Jianhua Wang for assistance with the NanoSIMS.

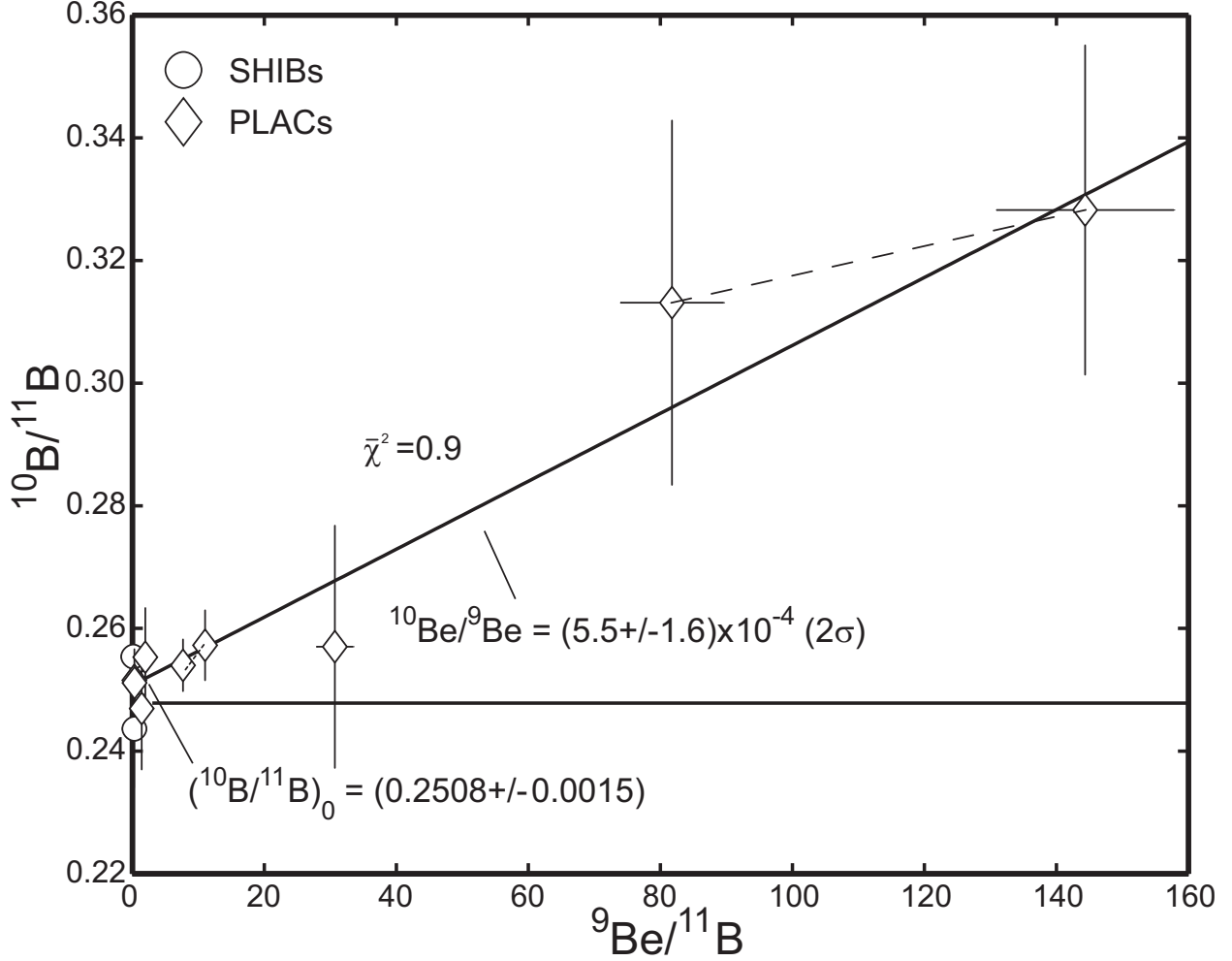


Fig. 1.—  $^{10}\text{Be}$ - $^{10}\text{B}$  isochron plot derived from the NanoSIMS analyses. Duplicated measurements on the same grains, which are connected with a dashed line, demonstrate good reproducibility. The PLACs show a significant range of Be/B ratios, which are strongly correlated with  $^{10}\text{B}$  excesses. The best fit to all the points yields  $^{10}\text{Be}/^9\text{Be} = 5.5 \times 10^{-4}$ . The horizontal solid line represents the chondritic  $^{10}\text{B}/^{11}\text{B} = 0.2476$ . Errors are  $2\sigma$ .

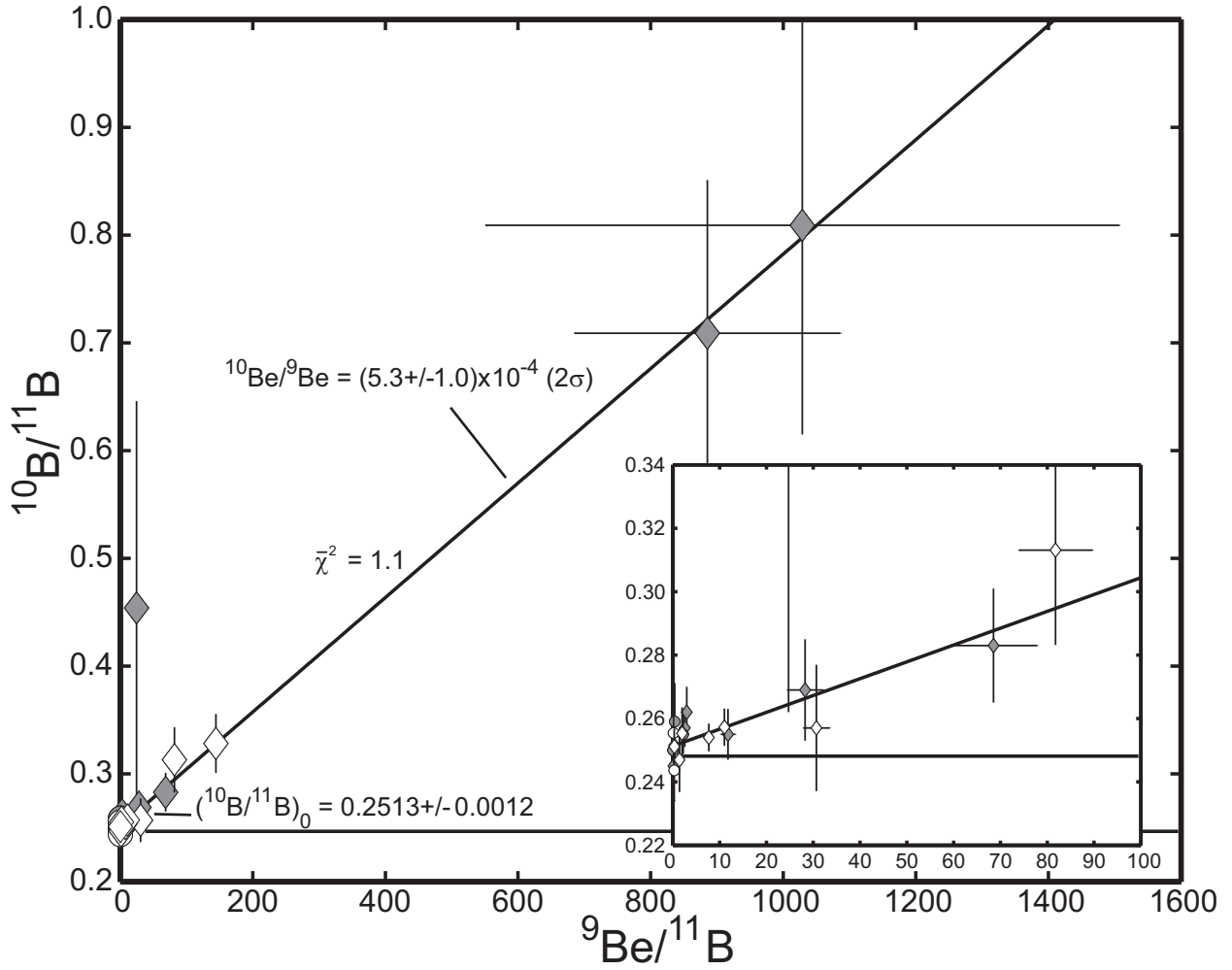


Fig. 2.— NanoSIMS results (open symbols) plotted with the data from Liu et al. (2009a) (filled symbols). An initial  ${}^{10}\text{Be}/{}^9\text{Be}$  ratio of  $(5.3 \pm 1.0) \times 10^{-4}$  is inferred from the data. The horizontal solid line represents the chondritic  ${}^{10}\text{B}/{}^{11}\text{B}$ . Errors are  $2\sigma$ .

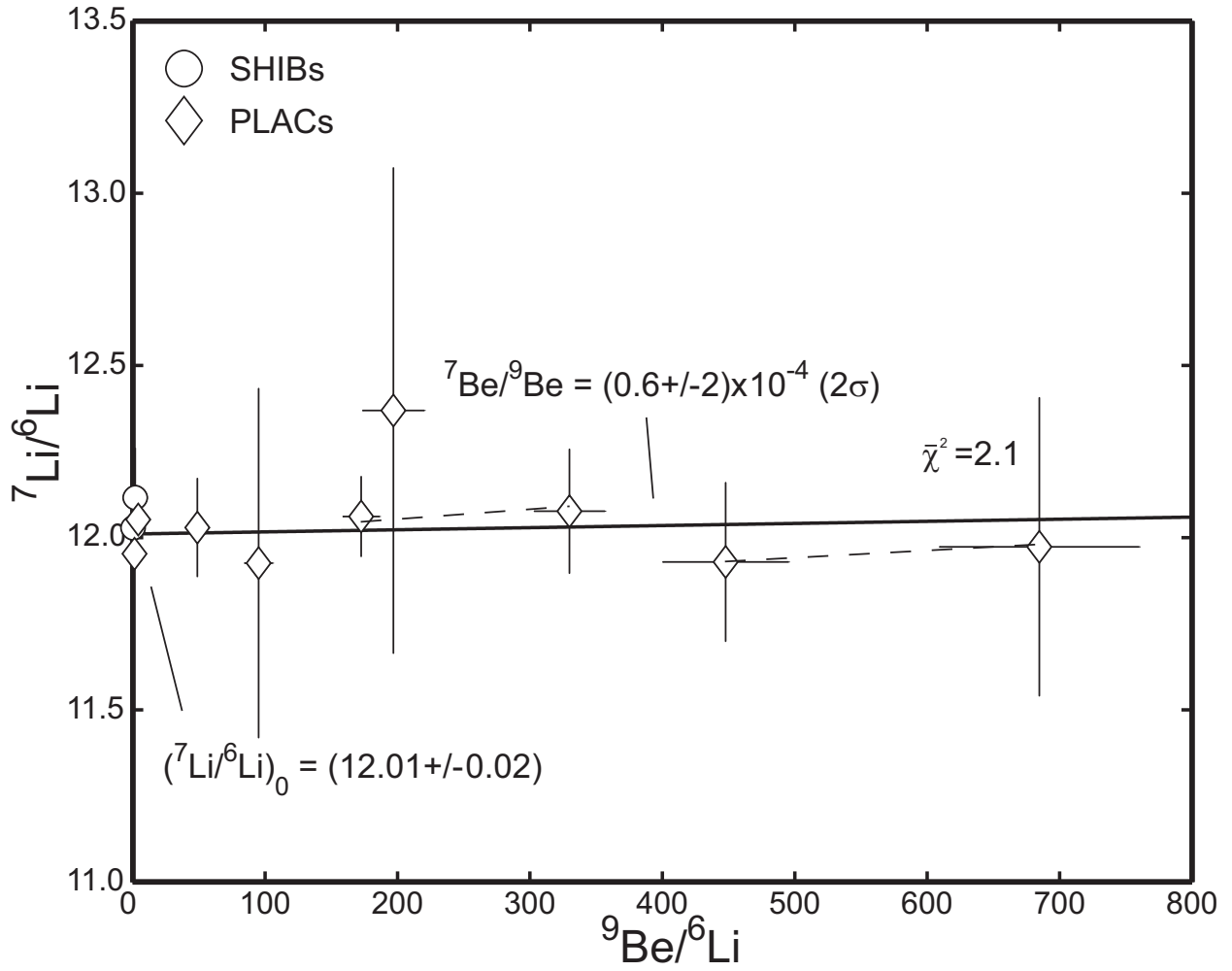


Fig. 3.—  ${}^7\text{Be}$ - ${}^7\text{Li}$  correlation plot. The  ${}^7\text{Li}/{}^6\text{Li}$  ratios in the grains are essentially chondritic ( $= 12.02$ ). Errors are  $2\sigma$ .

## REFERENCES

- Boss, A. 2008, *Earth Planet. Sci. Lett.*, 268, 102
- Chaussidon, M., Robert, F., & McKeegan, K. D. 2006a, *Geochim. Cosmochim. Acta*, 70, 224
- Chaussidon, M., Robert, F., & McKeegan, K. D. 2006b, *Geochim. Cosmochim. Acta*, 70, 5433
- Coogan, L. A., Kasemann, S. A., & Chakraborty, S. 2005, *Earth Planet. Sci. Lett.*, 240, 415
- Desch, S. J., Connolly, H. C. & Srinivasan, G. 2004, *ApJ*, 602, 528
- Fowler, W. A., Greenstein, J. L., & Hoyle, F. 1961, *American Journal of Physics*, 29, 393.
- Gounelle, M., Shu, F. H., Shang, H. Glassgold, A. E. Rehm, K. E. & Lee, T. 2001, *ApJ*, 548, 1051
- Gounelle, M., Shu, F. H., Shang, H. Glassgold, A. E. Rehm, K. E. & Lee, T. 2006, *ApJ*, 640, 1163
- Herzog, G. F., Vogt, S., Albrecht, A., Xue, S., Fink, D., Klein, J., Middleton, R., Weber, H. W. & Schultz, L. 1997, *Meteor. Planet. Sci.*, 32, 413
- Kasemann, S., Meixner, A., Rocholl, A., Vennemann, T., Rosner M., Schimitt, A. K. & Wiedenbeck M. 2001, *Geostan. Newslett. J. Geostan. Geoanal.*, 25, 405
- Koning, A. J., Hilaire, S., & Duijvestijn, M. C. 2005, in *AIP Conf. Proc.* 769, *International Conference on Nuclear Data for Science and Technology*, ed. R. C. Haight (New York: AIP), 1154
- Liu, M.-C., McKeegan, K. D., Goswami, J. N., Marhas, K. K., Sahijpal, S., Ireland, T. R. & Davis, A. M. 2009a, *Geochim. Cosmochim. Acta*, 73, 5051

- Liu, M.-C. & McKeegan, K. D. 2009b, *ApJ*, 697, L145
- Lodders, K. 2003, *ApJ*, 591, 1220
- MacPherson, G. J., Huss, G. R. & Davis, A. M. 2003, *Geochim. Cosmochim. Acta*, 67, 3165
- Marhas, K. K., Goswami, J. N. & Davis, A. M. 2002, *Science*, 298, 2182
- Marhas, K. K., & Goswami, J. N. 2003, *Lunar Planet. Sci. Conf.*, 34, 1303
- McDonough, W. F., Teng, F. Z., Tomascak, P. B., Ash, R. D., Grossman, J. N., & Rudnick, R. L. 2003, *Lunar Planet. Sci. Conf.*, 34, 1931
- McKeegan, K. D., Chaussidon, M., & Robert, F. 2000, *Science*, 289, 1334
- Michel, R., et al. 1997, *Nuclear Instruments and Methods in Physics Research B*, 129, 153
- Pearce, N. J. G., Perkins, W. T., Westgate, J. A., Gorton, M. P., Jackson, S. E., Neal, C. R. & Chenery, S. P. 1997, *Geostan. Newslett. J. Geostan. Geoanal.*, 25, 405
- Ramaty, R., Kozlovsky, B & Lingenfelter, R. E. 1996, *ApJ*, 456, 525
- Sahijpal, S., & Goswami, J. N. 1998, *ApJ*, 509, 137.
- Sisterson, J. M., Kim, K., Caffee, M. W., & Reedy, R. C. 1997, *Lunar Planet. Sci. Conf.*, 28, 1327
- Sugiura, N., Shuzou, Y. & Ulyanov, A. 2001, *Meteor. Planet. Sci.* 36, 1397
- Villeneuve, J., Chaussidon, M. & Libourel, G. 2009, *Science*, 325, 985
- Yiou, F., Maril, M., Dufaure de Citres, J., Fontes, P., Gradsztajn, E. & Bernas, R. 1968, *Phys. Rev.*, 166, 968

Zhai, M. Z., Nakamura, E., Shaw, D. M. & Nakano, T. 1996, *Geochim. Cosmochim. Acta*,  
60, 4877

Table 1. Results of Li-Be-B measurements in CM hibonites

Sample	$^9\text{Be}/^6\text{Li}$ ( $\pm 2\sigma$ )	$^7\text{Li}/^6\text{Li}$ ( $\pm 2\sigma$ )	$^9\text{Be}/^{11}\text{B}$ ( $\pm 2\sigma$ )	$^{10}\text{B}/^{11}\text{B}$ ( $\pm 2\sigma$ )	[Li]	[Be]	[B]
mt1-S1	0.29±0.03	12.03±0.08	0.14±0.01	0.2554±0.0092	476	14	150
mt3-S6	2.0±0.2	12.12±0.14	0.31±0.03	0.2436±0.0100	113	22	107
mt2-P12	95.1±10.7	11.93±0.51	0.31±0.03	0.2516±0.0051	6	53	255
mt3-P3	196.9±23.3	12.37±0.70	1.4±0.1	0.2469±0.0100	21	409	433
mt3-P4	48.8±5.1	12.03±0.14	30.7±2.8	0.2570±0.0200	105	511	25
mt3-P13@1	447.8±47.6	11.93±0.23	144.3±13.4	0.3282±0.0269	13	565	6
mt3-P13@2	684.7±75.5	11.97±0.43	81.7±7.84	0.3131±0.0297	9	601	11
mt4-P4@1	172.6±13.9	12.06±0.12	7.7±0.1	0.2540±0.0042	48	819	159
mt4-P4@2	329.8±26.8	12.08±0.18	11.0±0.2	0.2573±0.0057	24	784	106
mt4-P5	1.3±0.1	11.95±0.04	2.0±0.1	0.2553±0.0080	587	79	60
mt4-P8	4.2±0.3	12.05±0.04	0.33±0.01	0.2511±0.0019	487	205	929
Below are the data from Liu et al. (2009a)							
Mur-S7	0.12±0.01	11.96±0.04	0.05±0.02	0.2501±0.0040	6096	57	1526
Mur-S15	6.4±0.6	11.37±0.17	0.42±0.09	0.2589±0.0126	60	29	121
Mur-P1	1575.2±83.1	12.09±0.30	28.3±3.8	0.2690±0.0157	6	753	33
Mur-P2	3.5±0.1	11.98±0.10	24.7±9.0	0.4541±0.1915	95	26	2
Mur-P3	19.2±1.7	12.02±0.19	0.14±0.02	0.2446±0.0138	32	43	533
Mur-P6	3.5±0.1	11.87±0.04	3.0±0.4	0.2615±0.0076	2322	634	272
Mur-P7@1	543.2±40.2	11.63±0.23	1028.7±477.9	0.8087±0.1934	17	677	1
Mur-P7@2	1266.1±43.8	11.79±0.44	885.5±200.5	0.7088±0.1420	7	651	1
Mur-P8	213.7±27.7	11.72±0.12	68.5±9.3	0.2830±0.0187	43	609	11
Mur-P9	342.2±30.8	11.76±0.23	11.8±1.5	0.2551±0.0078	32	723	73
Mur-P10@1	370.9±12.4	12.15±0.41	2.6±0.3	0.2568±0.0067	20	570	262
Mur-P10@2	166.6±7.7	12.02±0.16	2.2±0.4	0.2550±0.0053	52	645	452

<sup>a</sup>[Li], [Be], and [B] are in unit of ppb (parts per billion)

<sup>b</sup>The letters “S” and “P” indicate SHIB and PLAC, respectively